The effects of anode material type on the optoelectronic properties of electroplated CdTe thin films and the implications for photovoltaic application

ECHENDU, O. K., DEJENE, B.F. and DHARMADASA, I
<http://orcid.org/0000-0001-7988-669X>

The effects of anode material type on the optoelectronic properties of electroplated CdTe thin films and the implications for photovoltaic application

O. K. Echendu[*a, b], B. F. Dejene[a] and I. M. Dharmadasa[b]

[a]Department of Physics, University of the Free State, Qwa Qwa Campus, Private bag X13, Phuthaditjhaba, 9866, South Africa.

[b]*Materials and Engineering Research Institute, Sheffield Hallam University, S1 1WB, Sheffield, United Kingdom.*

**Corresponding author e-mail address: oechendu@yahoo.com* *Tel:* +27(0)848831818

Abstract

The effects of the type of anode material on the properties of electrodeposited CdTe thin films for photovoltaic application have been studied. Cathodic electrodeposition of two sets of CdTe thin films on glass/fluorine-doped tin oxide (FTO) was carried out in two-electrode configuration using graphite and platinum anodes. Optical absorption spectra of films grown with graphite anode displayed significant spread across the deposition potentials compared to those grown with platinum anode. Photoelectrochemical cell result shows that the CdTe grown with graphite anode became p-type after post-deposition annealing with prior $CdCl_2$ treatment, as a result of carbon incorporation into the films, while those grown with platinum anode remained n-type after annealing. A review of recent photoluminescence characterisation of some of these CdTe films reveals the persistence of a defect level at (0.97 - 0.99) eV below the conduction band in the bandgap of CdTe grown with graphite anode after annealing while films grown with platinum anode showed the absence of this defect level. This confirms the impact of carbon incorporation into CdTe. Solar cell made with CdTe grown with platinum anode produced better conversion efficiency compared to that made with CdTe grown using graphite anode, underlining the impact of anode type in electrodeposition.

.

Keywords: Graphite anode; platinum anode; electrodepostion; carbon; conductivity type; CdTe solar cell.

1. **Introduction**

CdTe is a II-VI semiconductor with certain interesting properties that make it useful in areas of application such as radiation detectors [1] and solar cells [1, 2]. Some of these properties include its high absorption coefficient of $10^4 – 10^5$ cm^{-1} in the near-infrared to visible regions of the solar spectrum [3, 4], its near ideal energy bandgap of 1.45 eV for thin film solar cell application [3, 4], its conductivity mode dependence on stoichiometry, which makes it possible to be grown in n-type, i-type and p-type conductivity modes without introducing external dopants [5, 6], its Fermi level pinning behaviour due to native defects [7] and so on. Several growth techniques can

be applied in the growth of crystalline CdTe in both bulk and thin film forms. These include; physical vapour deposition [8], sputtering [9], close space sublimation (CSS) [10] and electrodeposition [11] to mention a few.

Electrochemical deposition, or simply electrodeposition, has been an interesting growth technique especially for thin film CdTe and CdTe-based solar cells since the 1970s with the work by Panicker and co-workers [12] as well as in the 1980s with the work of Basol and co-workers [1, 13]. The manufacturability of electrodeposition as a large-scale thin film solar cell fabrication technique has already been demonstrated by BP Solar in the late 1990s with the manufacture of CdTe-based solar panels of 0.94 m^2 area and 10.4% conversion efficiency [2]. Since this landmark achievement by BP Solar, interest in laboratory research on CdTe-based solar cell in general, based on various techniques, has grown considerably. As a result, the record efficiency of CdTe solar cell has increased rapidly in recent times from 16.5% [14] to 22.1% [15] for lab-scale cells and from 10.4% [2] to 18.6% [16] for modules, from 2001 to 2016, with First Solar, United States, taking the lead. This recent progress has triggered further interest in CdTe research, especially for thin film solar cell application, shedding more light on the understanding of this interesting material for improved device performance. The major improvement that led to the current record efficiencies of CdTe solar cell by First Solar has been attributed to improvement of carrier lifetime. This no doubt, has to do with elimination of defects (or trap centres) in the lattice (or rather bandgap) of CdTe in addition to improvement of crystallinity and grain-boundary passivation, among others. The issue of elimination of defects or trap centres in the bandgap of CdTe is of paramount importance in CdTe solar cells due to the undesirable carrier recombination effect and Fermi level pinning phenomenon which these defects can bring about.

In electrochemical deposition, external impurities can gain access into the deposited semiconductor through the chemical precursors used, when they are not of sufficient purity or more still, through the electrodes used in the deposition set-up. A faulty or broken Ag/AgCl or $Hg/HgCl_2$ reference electrode, for example, can result in the gradual leaching of the KCl or AgCl electrolyte of the electrode into the deposition electrolyte/bath and can result in incorporation of K^+ and Ag^+ into the semiconductor. In the case of CdTe in particular, these ions can pose a real problem, especially when an n-type CdTe is meant to be deposited, as they are known to constitute p-type (acceptor) dopants in CdTe [17]. This is more so as semiconductor doping takes place at parts per million (ppm) levels in general. Again, gradual dissolution of the anode material in the acidic deposition electrolyte can result in the incorporation of unwanted ions or atoms from the anode material into CdTe. This is possible since electrodeposition is mostly carried out in acidic medium with pH in the range of 1.50 – 2.50. Although inert metals (such as platinum) or non-metals (such as graphite) are mostly used as anode (counter electrode) materials in electrodeposition, their prolonged contact with the acidic electrolyte, which is sometimes heated to temperatures up to 90 °C, can lead to their very gradual dissolution into the deposition electrolyte. Through this means, undesired external impurities could get incorporated into electrodeposited CdTe. The impact of these incorporated impurities will depend on the

nature of the dissolved anode material (that is, dissolved impurity ions), the rate of dissolution of the anode material and the rate of its incorporation of the dissolved ions into the deposited CdTe material. This can have serious implications on solar cells or other devices made with such contaminated CdTe material. In this work, the authors have studied the impact of the two major anode materials – graphite and platinum- used in electrodeposition of semiconductors on the properties of deposited CdTe thin films and the possible implications on CdTe-based thin film solar cells fabricated with these CdTe materials.

2. Experimental procedure

For the electrodeposition of CdTe thin films, $CdSO_4$ (99.0% purity) and TeO_2 (99.999% purity), purchased from Sigma Aldrich, were used as precursors. The deposition electrolyte was made up of aqueous solution of 1.0 M $CdSO_4$ and 1 mM TeO_2 (with 1 mM each of high-purity $CdCl_2$ and CdF_2 to serve as sources of n-type dopants) in 800 ml of de-ionised water, all in 1000 ml plastic beaker. The pH of the electrolyte was adjusted to 2.00 using dilute sulphuric acid. The plastic beaker containing the electrolyte is in turn placed inside a 2000-ml pyrex glass beaker with some de-ionised water to serve as a water bath, and the electrolyte is stirred for 24 h using a magnetic stirrer. However, prior to the addition of TeO_2, $CdCl_2$ and CdF_2, the $CdSO_4$-only solution was heated to 85 °C on a hotplate with stirring for few hours. The solution was then subjected to cyclic voltammetry with cleaned glass/fluorine-doped tin oxide (FTO) as substrate (cathode) and platinum plate as anode (counter electrode) using a Gill AC Potentiostat/Galvanostat (ACM Instruments, UK) in two-electrode configuration, in order to determine the cathodic deposition potential of Cd. At a cathodic potential slightly less than the deposition potential of Cd, electro-purification of the $CdSO_4$ solution was carried out for 24 h because of the low purity of $CdSO_4$. This serves to remove metallic ions that may be present in the $CdSO_4$ powder. After this electro-purification step, TeO_2, $CdCl_2$ and CdF_2 were then added to the solution to obtain the above mentioned CdTe deposition electrolyte. Another set of cyclic voltammetry was carried out using the graphite and platinum anodes in turn in order to determine the range of deposition potentials for CdTe using the different anodes. Full details of the electrodeposition of CdTe thin films using graphite anode and platinum anode have been reported recently [6, 18]. The cathodic electrodeposition of two sets of CdTe thin films (of four samples per set), at different voltages, was carried out on glass/FTO (g/FTO) substrate using the same Gill AC Potentiostat/Galvanostat in two-electrode configuration. Each CdTe film was deposited for 1hour while maintaining the deposition current density steady. This ensures that equal thickness of CdTe is deposited. This is possible because for a given deposition time (t), the theoretical thickness (T) of an electrodeposited semiconductor film according to the Faraday's equation ($T = MtJ/nF\rho$) is known to be directly proportional to the deposition current density (J) [11, 18] with the rest of the parameters [molecular mass (M), number of electrons involved in the formation (n), Faraday's constant (F) and density of the material (ρ)] being constants for any given material. In

one set of the films deposited, graphite rod was used as anode material while platinum plate was used in the other set in order to study the effect of each of the anode materials on the properties of the CdTe thin films electroplated. Each CdTe in both sets was divided into two. One-half of each set was designated "as-deposited" while the other half was dipped in saturated solution of $CdCl_2$ in de-ionised water, dried and then annealed at 450 °C in air for 15 minutes. This set was designated "annealed". Both the as-deposited and annealed sets of samples were characterised for their structural, optical, electrical, morphological and compositional properties using X-ray diffraction (XRD), optical absorption, photoelectrochemical (PEC) cell, scanning electron microscopy (SEM) and energy dispersive X-ray (EDX) techniques respectively. Two solar cells of device structure g/FTO/CdS/CdTe/Au were fabricated each with CdTe grown at the best deposition voltage using graphite anode and platinum anode respectively. For the complete solar cell fabrication, the CdTe surfaces were etched with acidified $K_2Cr_2O_7$ and $NaOH+Na_2S_2O_3$, successively rinsed in de-ionised water each time and finally dried in a stream of N_2. Then Au metal contacts were evaporated onto the etched CdTe surfaces in a vacuum chamber as described previously [19, 20]. Performance of the devices was assessed using Keithley 619 Electrometer/multimeter under AM 1.5 condition for comparison.

3.0 Results and Discussion

3.1 X-ray diffraction study

Figures 1(a) and (b) show the XRD patterns of as-deposited CdTe thin films grown with graphite anode and platinum anode respectively.

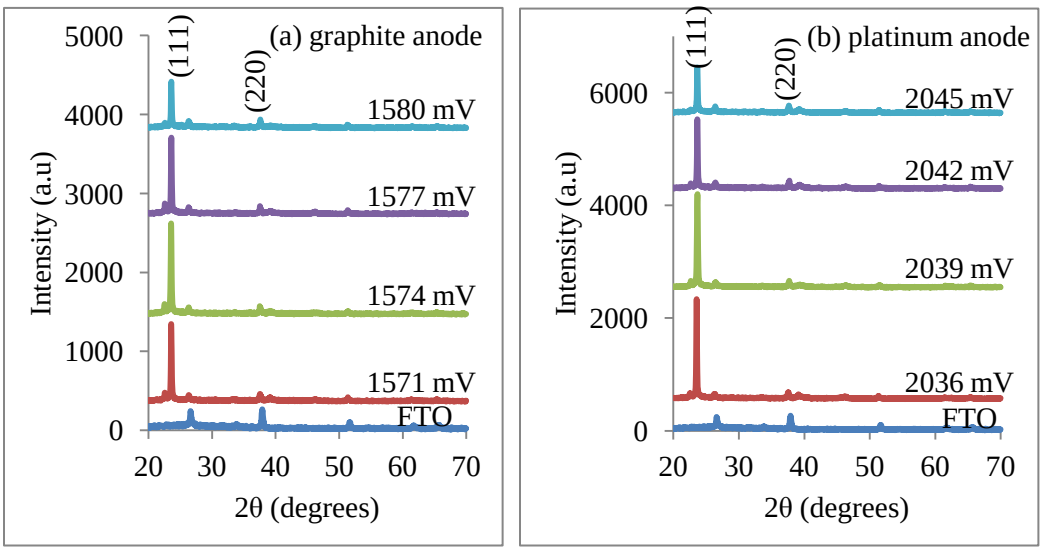

Figure 1: XRD patterns of as-deposited CdTe films grown at different cathode voltages with (a) graphite anode and (b) platinum anode.

In the as-deposited form the CdTe films grown with both graphite and platinum anodes display similar XRD patterns of cubic CdTe with only (111) and (220) diffraction peaks appearing at 2θ ~ 23.7° and ~39.2° respectively, and preferential orientation in the (111) crystal plane. These patterns agree with the Joint Committee on Power Diffraction and Standards (JCPDS) reference file no: 00-015-0770 for cubic CdTe. Important to note from the figures also is the fact that CdTe films of similar structural quality could be grown in a reasonably wide window of potentials (9 mV window in this case) using either counter electrode (anode) material.

Figures 2(a) and (b) also show the XRD patterns of the same samples found in figure 1 after post-deposition annealing with prior $CdCl_2$ treatment. This time, as is well known of post-deposition annealing of CdTe, improvement in crystallization of the films is witnessed through the emergence of additional peak from the (311) crystal plane at 2θ ~ 46.3°, as well as improvement in the intensities of the two previous peaks from (111) and (220) planes. The polycrystalline nature of the CdTe films from both graphite and platinum anodes therefore becomes more obvious. The improvement in the intensities of all three peaks is however observed to be more pronounced in the films grown with graphite anode. This is attributed to a combination of improvement in crystallinity and increase in the randomization of the crystallites which gives rise to increased tendency towards polycrystallinity in these materials.

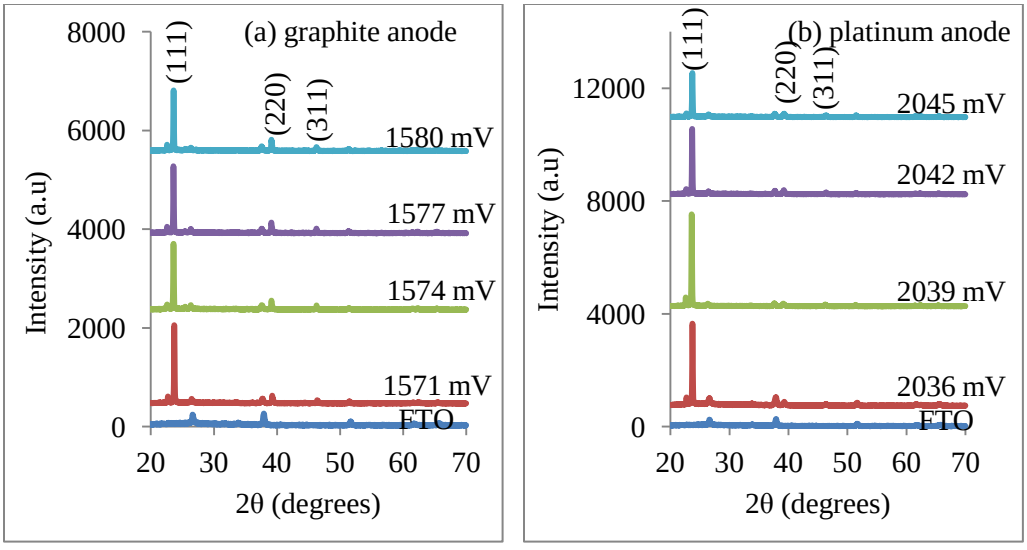

Figure 2: XRD patterns of annealed CdTe films grown with (a) graphite anode and (b) platinum anode.

Figure 3 shows the variation of the (111) peak intensity with both deposition potential and annealing for the CdTe grown with (a) graphite anode and (b) platinum anode. In both cases, one observes that the peak intensity appears to reach a maximum at a certain deposition potential and decreases afterwards beyond this potential. As pointed out earlier, figures 3(a) and (b) show that

post-deposition annealing increases the intensity of this peak beyond that of as-deposited film for the deposition potentials under consideration. Thus there is improvement in preferential orientation of the crystallites along this plane, for the conditions under study. An analysis of the (111) peak for CdTe grown with both graphite and platinum anodes shows similar results with 2θ = (23.6 – 23.7)°, inter-planar spacing = (3.75 – 3.77) Å, lattice constant = (6.40 – 6.48) Å, full width at half maximum = (0.1624 - 0.1299)° and crystallite size = (50 – 63) nm. These are in very good agreement with corresponding parameters of the JCPDS reference material which are: 2θ = 23.8°, inter-planar spacing = 3.74 Å and lattice constant = 6.48 Å.

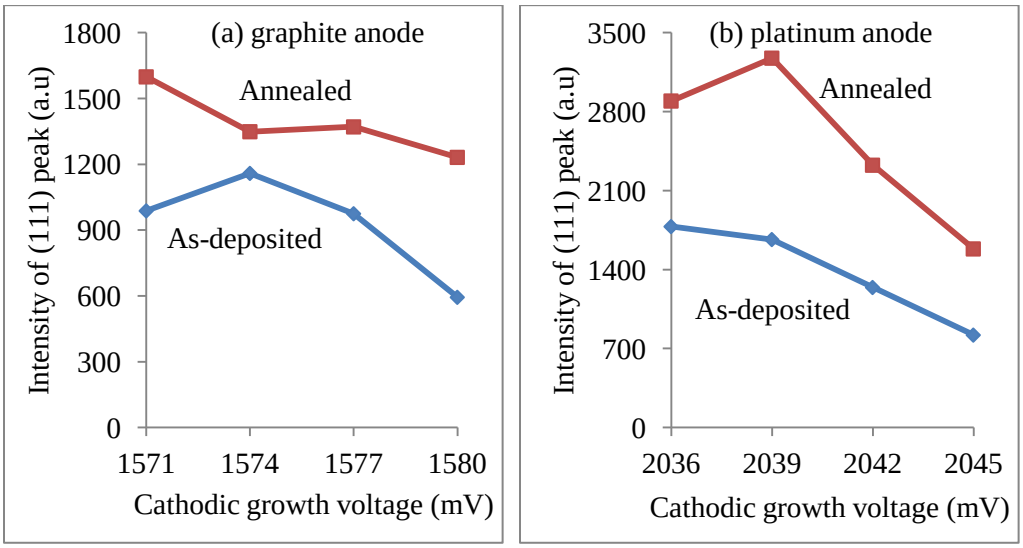

Figure 3: (111) XRD peak intensity vs. cathodic growth voltage for CdTe grown with (a) graphite anode and (b) platinum anode.

3.2 Optical absorption study

Figures 4(a) and (b) show the graphs of absorbance vs. photon wavelength for as-deposited CdTe films grown using graphite anode and platinum anode, respectively. The figures show at first that the set of four CdTe films for each anode material, display similar absorption behaviour with absorption edges in the neighbourhood of 800 nm. On a closer look, one also sees a slightly wider spread in the absorption curves of the CdTe grown with graphite anode compared to those grown with platinum anode.

In general again, one observes that the CdTe materials in figure 4(a) have slightly higher absorbance towards the ultra-violet (UV) region of the solar spectrum. This is also attributed to a combination of improvement in crystallinity and increase in the randomization of the crystallites (increase in polycrystallinity) in these materials. However, the major difference between the two

sets of CdTe under study begins to appear with this optical characterization. A wider spread/scatter in the optical properties is observed in the annealed samples in figure 5.

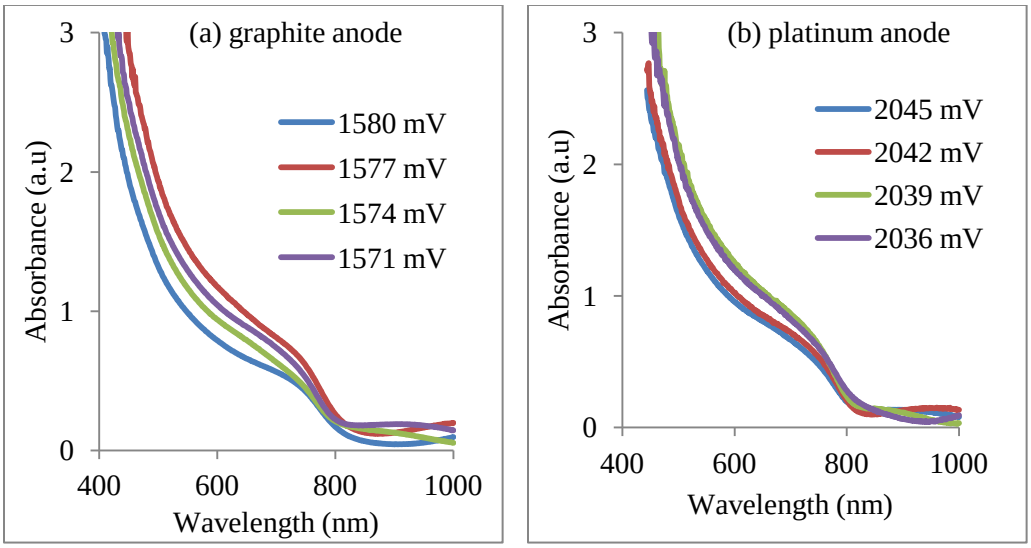

Figure 4: Absorbance vs. photon wavelength for as-deposited CdTe films grown with (a) graphite anode and (b) platinum anode.

Figure 5(a) shows unusual behavior in the absorbance of the CdTe grown with graphite anode. Two of the samples surprisingly display a sort of reduction and/or saturation in absorbance towards the UV region compared to their as-deposited form.

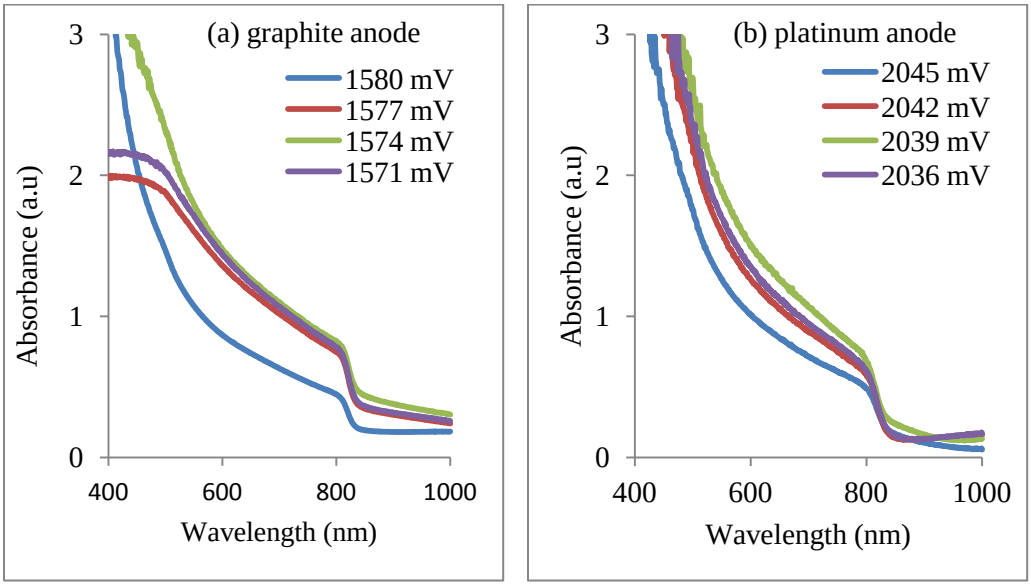

Figure 5: Absorbance vs. photon wavelength for annealed CdTe films grown with (a) graphite anode and (b) platinum anode.

This behavior is not seen in the samples grown with platinum anode in which case, one rather sees a general improvement in absorbance on annealing compared to the as-deposited forms.
This unusual behavior in the samples grown with graphite anode is attributed to possible incorporation of carbon atoms/ions into CdTe during the growth process. It can be recalled that Tkachuk *et al*.[21] has earlier in 2000 reported what they described as macro- and micro-inhomogeneities as well as carbon-related deep centres in semi-insulating CdTe(Cl) single crystals grown in graphitized quartz ampoules by melt growth technique. According to them, these negatively affected the detector performance of these crystals. These effects were not observed by the authors in the CdTe(Cl) crystals grown with non-graphitized quartz ampoules.

Figure 6 shows the graphs of square of absorbance vs. photon energy for the as-deposited CdTe grown with (a) graphite anode and (b) platinum anode. The graph of square of absorbance vs. photon energy is a very easy and quick way of estimating the energy bandgap of thin film semiconductors without actually going through Tauc plot which requires determination of film thickness and absorption coefficient. Our experience shows that both methods produce very similar values for the energy gap determined. Again figure 6(a) shows a wider spread in the absorption curves of the samples grown with graphite anode compared to those grown with platinum anode. This observed spread corroborates the observation in figures 4 and 5. Figures 6(a) and (b) however show as-deposited CdTe films from both systems to have a common energy bandgap of 1.55 eV.

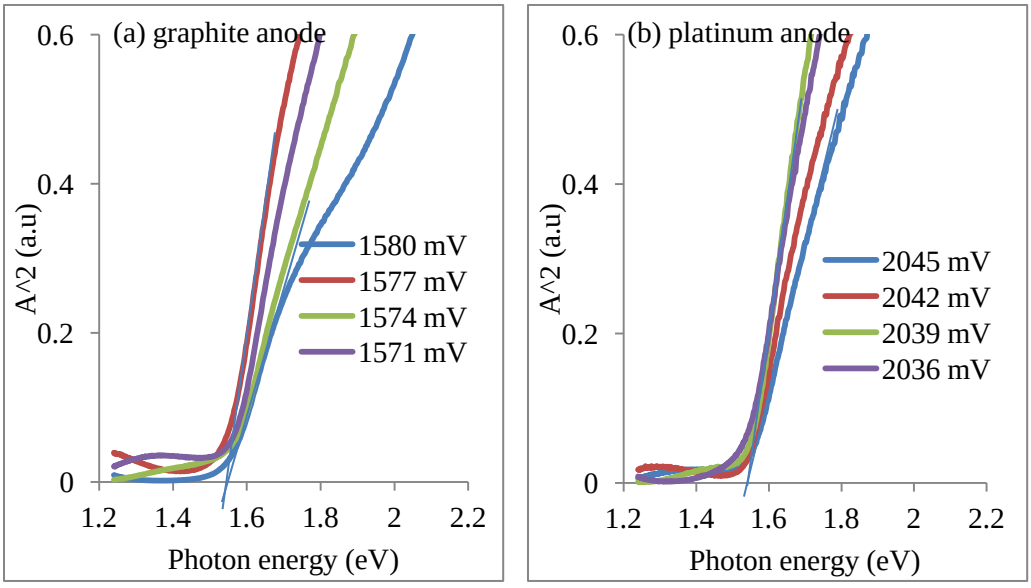

Figure 6: Square of absorbance vs. photon energy for as-deposited CdTe films grown with (a) graphite anode and (b) platinum anode.

After annealing, figures 7(a) and (b) show that all the CdTe from both systems also have common reduced bandgap of ~1.48 eV. However, again, the samples grown with graphite (figure 7(a)) still show wide spread in the absorption, across the entire photon energy range. This situation suggests the presence of trap centres in the bandgap of these particular CdTe samples due to the incorporation of carbon atoms/ions into the CdTe films. These atoms create defect/trap centres in the bandgap of CdTe and these defects tend to get activated by the annealing process.
Another important feature arising from figures 7(a) and (b) on close observation is the highest gradient of these absorption curves for the films grown at cathodic voltages of 1574 mV (with graphite anode) and 2039 mV (with platinum anode). These curves become closer to vertical absorption edges, indicating minimization of defects in the bandgap of the materials. Again, the absorption edges of the films grown with platinum anode are better than those of the films grown with graphite anode.

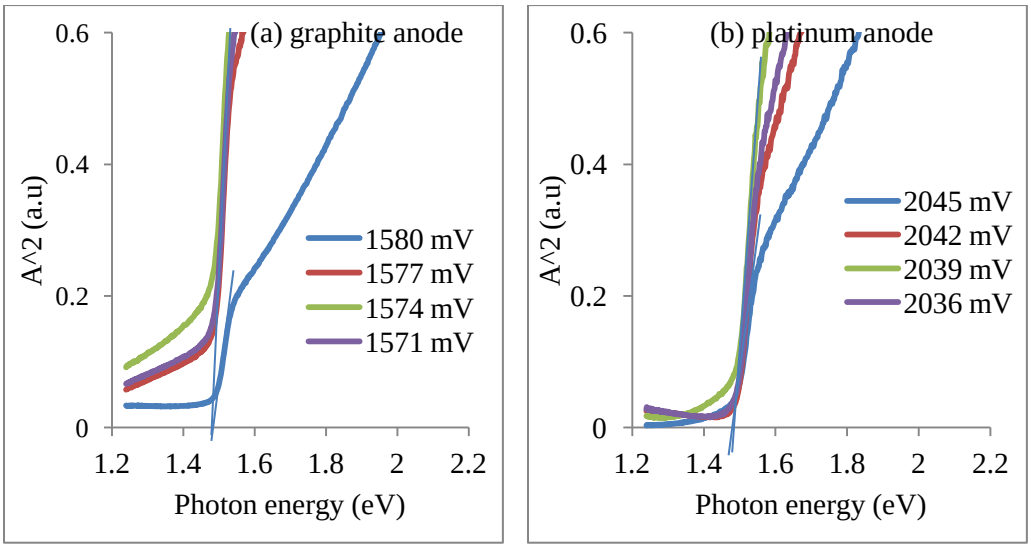

Figure 7: Square of absorbance vs. photon energy for annealed CdTe films grown with (a) graphite anode and (b) platinum anode.

3.3 Photoelectrochemical (PEC) cell study

Tables 1 and 2 show the results of photoelectrochemical (PEC) cell signal measurements on the CdTe thin films grown with graphite anode and platinum anode respectively, for the determination of conductivity types of the electrodeposited CdTe materials. It is important here to state that well-known techniques such as Hall Effect measurements could not be used to determine the conductivity types of these films mainly because they are grown on conducting FTO substrates. The application of Hall Effect will result in the diversion of electric current through the FTO layer which is a path of least resistance in this case. This will no doubt interfere

with the result obtained. This is more so as it is extremely difficult to detach the electrodeposited CdTe layers from the FTO substrates. As a result, we use PEC signal measurement in our group. This rather uses the underlying conducting FTO as an electrode, with graphite as the second electrode. The basic principle of the PEC cell measurement for the determination of conductivity type of semiconductors has been described in recent publications [22, 23]. However, the technique principally involves the formation of a liquid/solid junction at the interface between the thin film under study and an appropriate electrolyte. The liquid/solid junction is essentially a Schottky barrier junction in which the direction of band-bending in the semiconductor at the interface depends on the conductivity type of the semiconductor. A built-in potential develops in the depletion region formed. The value of this built-in potential varies under illumination. What is very important here is the PEC signal which is the difference between the voltages measured under illumination (V_L) and under dark (V_D) conditions. The magnitude of this PEC signal (V_L-V_D) indicates the quality of the depletion layer formed at the semiconductor-electrolyte interface. The PEC signal also indicates the doping level of the material under study. The sign of the PEC signal determines the conductivity type of the material. Both insulating and heavily doped layers show zero PEC. The system must however be calibrated using semiconductors with known conductivity types to avoid error. In the system we used, which was properly calibrated using well-known n-CdS and p-ZnTe materials, aqueous solution of 0.1 M $Na_2S_2O_3$ was used as an electrolyte and a graphite rod as an electrode. The FTO layer on which CdTe material is grown serves as the second electrode. In this system, a positive PEC signal indicates a p-type semiconductor while a negative PEC signal indicates an n-type semiconductor. It may be of interest also to mention that there are other PEC measurement approaches which involve carrying out cyclic voltammetry and doing Mott-Schottky plot in order to determine the conductivity type of a semiconductor [24, 25]. These approaches however, are outside the scope of this work reported in this paper.

Table 1: PEC cell results of as-deposited and annealed CdTe layers grown using the two-electrode system with graphite anode.

	As-deposited				Annealed			
Vg (mV)	V_D (mV)	V_L (mV)	PEC (V_L-V_D) (mV)	Type	V_D (mV)	V_L (mV)	PEC (V_L-V_D) (mV)	Type
1571	-210	-277	-67	**n**	-121	-49	+72	**p**
1574	-240	-382	-142	**n**	-98	-28	+70	**p**
1577	-168	-222	-54	**n**	-135	-39	+96	**p**
1580	-190	-261	-71	**n**	-112	-33	+79	**p**

Table 2: PEC cell results of as-deposited and annealed CdTe layers grown using two-electrode system with platinum anode.

	As-deposited				Annealed			
Vg (mV)	V_D (mV)	V_L (mV)	PEC (V_L-V_D) (mV)	Type	V_D (mV)	V_L (mV)	PEC ($V_L V_D$) (mV)	Type
2036	-250	-427	-177	**n**	-96	-146	-50	**n**
2039	-254	-425	-171	**n**	-73	-116	-43	**n**
2042	-156	-329	-173	**n**	-75	-84	-09	**n**
2045	-163	-315	-153	**n**	-88	-144	-56	**n**

The results in Tables 1 and 2 show that the CdTe films in their as-deposited form are all n-type in electrical conduction for both anode types. After annealing however, all of the films grown with graphite anode became p-type in electrical conduction (Table 1) while those grown with platinum anode remained n-type (Table 2). As mentioned earlier, annealing at 450 °C for 15 minutes must have activated the carbon atoms, or any other impurities from the graphite electrode, which were already incorporated into these CdTe films during deposition. The source of incorporated impurities may likely be carbon atoms and impurities that may have gradually leached into the acidic deposition electrolyte from the graphite anode. The removed carbon from the electrode is sometimes observed as black powder at the bottom of the beaker containing the deposition electrolyte when the graphite anode is used for a long time. The incorporation of carbon atoms into CdTe is possible owing to the very small atomic and ionic radii of carbon compared with Cd, Te and Pt as can be seen in Table 3. Incorporation of Pt would rather be more difficult given its very large atomic and ionic radii compared to carbon. For carbon, the very small size makes it possible to be incorporated most likely as interstitial impurity into CdTe.

Table 3: Atomic properties of carbon, cadmium, tellurium and platinum [26].

Element	**Atomic number**	**Atomic radius (Å)**	**Ionic radius (Å)**
C	6	0.67	0.70
Cd	48	1.61	1.55
Te	52	1.23	1.40
Pt	78	1.77	1.35

Although Pt is known to be stable at high temperatures, its prolonged contact with hot acidic deposition electrolyte, in the presence of certain atomic species like sulphur and halogens, could result to its gradual corrosion. It therefore becomes possible that Pt atoms could eventually find their way into the electrodeposited semiconductor, a situation which could also affect the properties of such semiconductor and the devices made with it. In any case, it is advisable, as a

precaution, to minimize the contact time of these electrodes in the deposition electrolyte. This can be achieved by ensuring that the electrodes only make contact with the electrolyte during deposition, and immediately washing and storing them in a safe place after use.

It is important at this point to state that the observed conductivity type change for the CdTe grown with graphite anode is most likely due to carbon incorporation and not due to the conductivity type conversion well known to take place in CdTe at times after post-deposition annealing with prior $CdCl_2$ treatment. This becomes important to note as the deposition electrolyte *ab initio* contains Cl and F for n-type doping of CdTe and we had recently shown that CdTe films grown from this electrolyte retain their n-type conductivity after post-deposition annealing with prior $CdCl_2$ treatment [27]. Although the graphite rods have been purchased as "high-purity graphite", their impurity contents are not known to the research community. Therefore this discussion is only limited to the possible incorporation of carbon into electroplated CdTe layers.

A review of photoluminescence (PL) study at 80 K, of a set of CdTe thin films grown in 2-electrode configuration with graphite and platinum anode, as well as with different Cd precursors by the authors, show that CdTe films grown with graphite anode, in 2-electrode configuration, tend to uniquely retain a defect level at (0.97 – 0.99) eV below the conduction band minimum of CdTe after post-deposition annealing with prior $CdCl_2$ treatment, compared to CdTe films grown with platinum anode (see Table 4) [28]. Table 4 shows a summary of the PL results [28] in which all the CdTe films electrodeposited from different Cd precursors and using the two different anodes have the four identified defect levels. After annealing however, the defect level at T_1 (0.66 eV) below the bottom of the conduction band is completely removed from all the CdTe samples irrespective of the anode materials and Cd precursor used. Strikingly too, the defect level at T_3 (0.97 – 0.99) eV below the bottom of the conduction band is completely eliminated from the CdTe film grown with platinum anode, while for all the CdTe films grown with graphite anode, the same defect level persists. This level is therefore most likely related to carbon impurities from the graphite anode incorporated into the deposited CdTe. This corroborates the results observed in the optical and PEC results of these materials as well as the observations of Tkachuk *et al.* cited earlier in ref [21]. The defect level observed at (1.38 – 1.40) eV in both CdTe grown with graphite and platinum anodes must be related to native defects in CdTe irrespective of the Cd precursor and anode material used in the deposition.

A combination of the PEC and PL results indicates that the presence of carbon atoms in the CdTe grown with graphite anode tends to cause the movement of the Fermi level of the CdTe towards the valence band edge in the post-deposition annealing process as indicated in figure 8 (a), thereby making the material display p-type conductivity. This situation is also most likely encouraged by the Fermi level pinning phenomenon that is well-known to be pronounced in CdTe [29].

Table 4: Summary of defect levels observed in electrodeposited CdTe thin films using photoluminescence study at 80 K for CdTe grown using graphite anode and platinum anode [28].

Cd precursor and anode type	**Nature of CdTe**	**Defect levels identified**				
		T_1 (eV)	T_2 (eV)	**T_3 (eV)**	T_4 (eV)	E_g (eV)
$CdSO_4$ (Platinum)	As-Deposited	0.66	0.77	**0.97**	1.36	1.51
	$CdCl_2$ treated	----	0.73	**----**	1.39	1.47
$CdSO_4$ (Graphite)	As-Deposited	0.66	0.79	**0.97**	1.37	1.50
	$CdCl_2$ treated	----	0.74	**0.97**	1.38	1.48
$Cd(NO_3)_2$(Graphite)	As-Deposited	0.66	0.79	**0.98**	1.37	1.50
	$CdCl_2$ treated	----	0.71	**0.99**	1.40	1.48

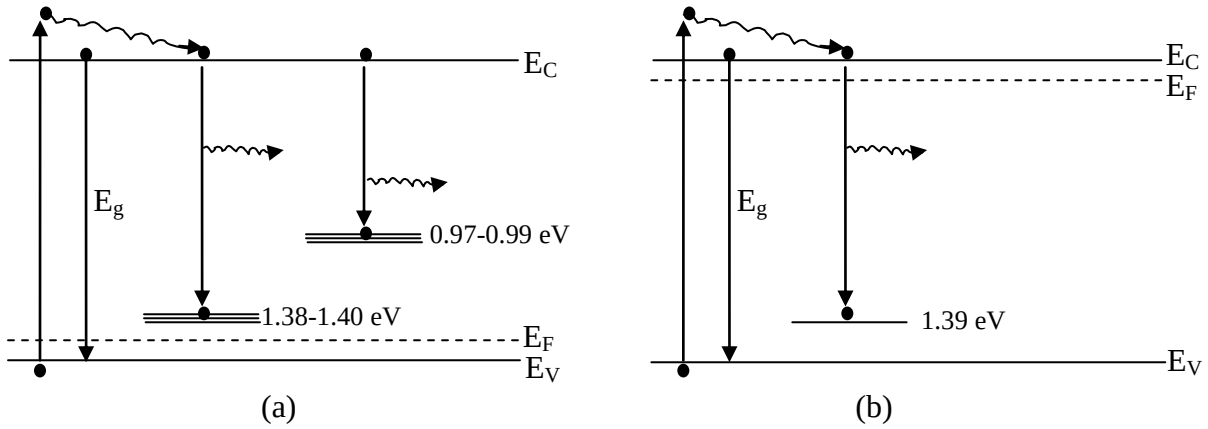

Figure 8: Energy band diagrams showing energy level transitions in the photoluminescence measurements of CdTe grown with (a) graphite anode and (b) platinum anode following post-deposition annealing.

The persistent deep level at (0.97 – 0.99) eV as shown in Table 4 and figure 8 (a) could act as detrimental recombination center for photo-generated electrons when these CdTe materials are used for solar cell fabrication thereby producing solar cells with poor performance. It can also pin the Fermi level of the CdTe at that level thus limiting the barrier height formed at the CdTe/metal interface and therefore adversely affect device performance. This situation will become very clear from the performance of solar cell fabricated with these CdTe materials later.

3.4 Scanning electron microscopy and energy dispersive x-ray studies

Figures 9(a) and (b) show the typical SEM images of electrodeposited CdTe thin films grown on glass/FTO/CdS substrates using graphite anode and platinum anode, respectively. Only these two images are presented since all the SEM images look alike. The images show tiny nano-particulate CdTe crystallites coalescing into larger agglomerates in both cases. A good coverage of the underlying substrate by the compact agglomerates is also evident.

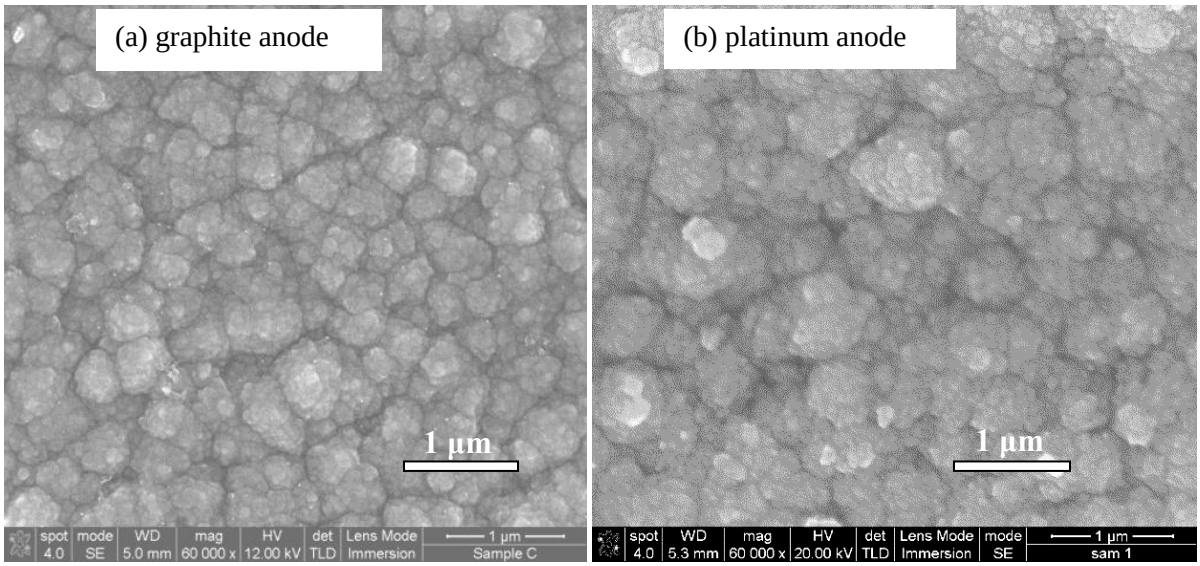

Figure 9: Typical SEM images of CdTe films grown using (a) graphite anode and (b) platinum anode.

Figures 10(a) and (b) also show the representative EDX spectra of CdTe grown on glass/FTO/CdS substrates with graphite anode and platinum anode, respectively. Again only two representative EDX spectra are presented since others are very similar. Both figures indicate the presence of Cd and Te in the CdTe layers grown with graphite and platinum anodes. The two spectra also show the presence of S from the underling CdS on which the CdTe layers were grown. The peak assigned to carbon in the lower energy region of the EDX spectrum for CdTe grown with graphite anode may however be misleading as an evidence of carbon incorporation into CdTe. This is because, apart from the fact that this peak and the other peaks around it also correspond to peak positions for N, O, Cd, Te and C, EDX is not known to be a very accurate technique for the detection of small amounts of atoms, especially at doping levels which occur in parts per million levels. For this reason, the EDX spectra in figure 10 will not be used as a confirmatory result for the presence of carbon atoms in the electrodeposited CdTe films.

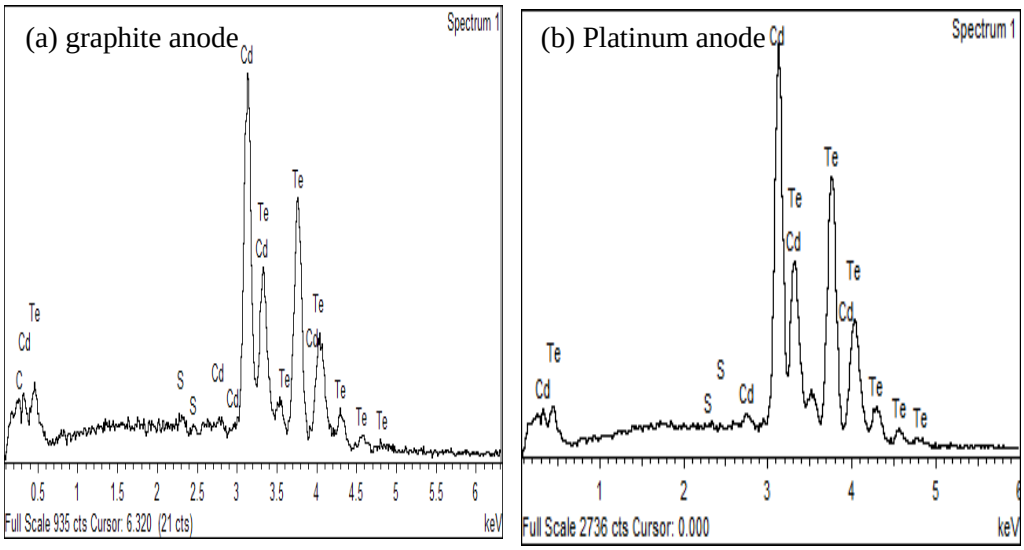

Figure 10: Typical EDX spectra of CdTe thin films grown on g/FTO/CdS with (a) graphite anode and (b) platinum anode.

3.5 G/FTO/CdS/CdTe/Au Solar cell performance assessment

Figures 11 (a) and (b) show the current density-voltage graphs of the best g/FTO/CdS/CdTe/Au solar cells fabricated with CdTe grown at 1577 mV and 2039 mV using graphite anode and platinum anode respectively. These two deposition voltages were chosen by considering both the results presented in this work and the results of our previous work on electrodeposited CdTe materials using both graphite and platinum anodes. This is necessary as it becomes a bit difficult to give a straightforward verdict on the best growth voltage for each anode type from the results presented already in this work. However, in our previous but recent careful work on the best deposition voltages for CdTe using graphite anode as well as platinum anode, we have reported 1576 mV as the best deposition voltage using graphite anode [6, 11], and 2038 mV as the best deposition voltage for CdTe using platinum anode [18 - 20]. Based on this, we then decided to choose 1577 mV and 2039 mV as the deposition voltages of choice for graphite anode and platinum anode, respectively for the fabrication of the solar cells presented in figure 11. These two voltages are the closest to the already established best voltages based on our recent work in this direction. The solar cell open-circuit voltage (V_{oc}), short-circuit current density (J_{sc}), fill factor (FF), efficiency (η) and series resistance (R_s) extracted from the two graphs are 470 mV, 29.2 $mAcm^{-2}$, 0.33, 4.5% and 253 Ω respectively for figure 11(a) and 660 mV, 33.6 $mAcm^{-2}$, 0.38, 8.4% and 107 Ω respectively for figure 11(b). These device results show that the CdTe grown with platinum anode produces solar cells with better overall conversion efficiency compared to that grown with graphite anode. For the device involving CdTe grown with graphite anode (figure 11 (a)), the Fermi level of the CdTe may have been pinned at one of the two available defect level bands (0.97-0.99 eV and 1.38-1.40 eV) in figure 8(a) and Table 4. It is

important here to mention that the CdTe surface treatment employed prior to Au back contact formation (i.e etching in acidified oxidizing $K_2Cr_2O_7$ etch, and then in reducing NaOH+$Na_2S_2O_3$ etch) is known to produce Cd-rich surface in which the Fermi level is pinned close to the valence band maximum, resulting in devices with better performance for both n-CdTe and p-CdTe [19,30, 31].

Considering the PEC results in which we have both n-type and p-type CdTe after annealing and figure 8, pinning of the Fermi level at the 1.38 – 1.40 eV defect level would produce equally good solar cells with both CdTe materials, since this situation will give rise to good ohmic contact at the p-CdTe/Au interface (combined with p-n heterojunction at n-CdS/p-CdTe interface) and a good Schottky barrier at the n-CdTe/Au interface (combined with n-n heterojunction at n-CdS/n-CdTe interface). This is however not evident in the solar cell results obtained. Whereas the n-CdTe-based device produced good solar cell parameters as expected, the type-converted p-CdTe-based device did not. This shows that actually, a good Schottky barrier is produced in the n-CdTe–based solar cell therefore producing the relatively higher V_{oc}, J_{sc}, FF, η and lower R_s. This is possible since only one defect level (1.39 eV) is present in this CdTe and close to the valence band edge therefore making Fermi level pinning highly probable at this level. This particular device structure of g/FTO/n-CdS/n-CdTe/Au n-n heterojunction + Schottky barrier is known to produce solar cells with high short-circuit current density as observed here, due to a possible combination of two depletion regions at both the n-n heterojunction and at the Schottky junction [19, 20, 32]. This situation creates a combined wide depletion region in the device. This, coupled with the well-known characteristic fast response of Schottky barrier devices (a property that makes them preferable in fast switching circuits), gives rise to effective collection of photo-generated charge carriers and therefore high J_{sc} values.

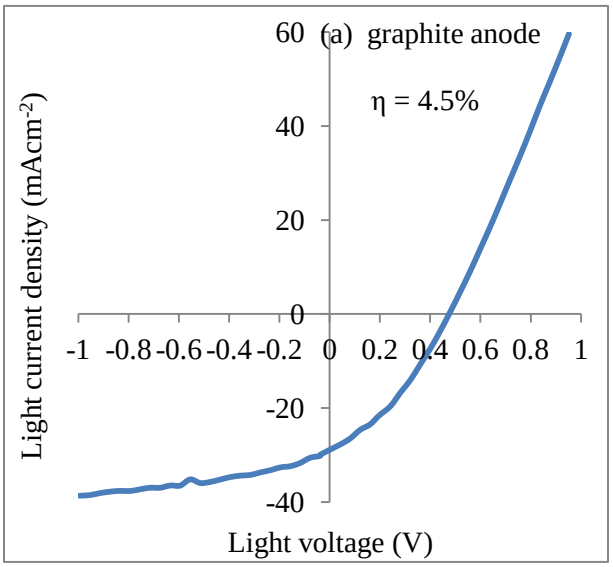

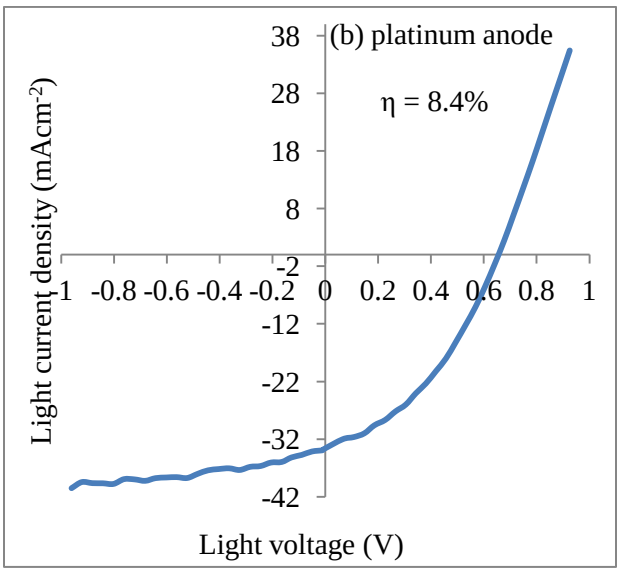

Figure 11: AM 1.5 Current density-voltage graph of g/FTO/CdS/CdTe/Au thin film solar cell fabricated with CdTe grown with (a) graphite anode and (b) platinum anode.

On the other hand, if the Fermi level is pinned at the defect level with 0.97 – 0.99 eV (a situation which is only available in the CdTe grown with graphite anode), this will produce a low Schottky barrier height (or a poor ohmic contact) at the p-CdTe/Au interface, since a given metal which produces a large Schottky barrier on an n-type semiconductor will produce a low Schottky barrier height in a p-type of the same semiconductor [31, 33]. Such poor Schottky barrier or a poor ohmic contact will give rise to low V_{oc}, J_{sc}, FF, η and high R_s which is the case with the solar cell made with CdTe produced using graphite anode in figure 11(a). This situation therefore indicates that the presence of the defect levels at 0.97 – 0.99 eV is detrimental to CdS/CdTe-based devices by producing devices with poor parameters.

4. Conclusion

This work clearly shows that better optoelectronic properties and therefore solar cell performance, are obtained when CdTe layers are electroplated using platinum anode in two-electrode configuration than using graphite anode. The use of graphite anode in the electrodeposition of semiconductors could result in micro-inhomogeneity and formation of deep centers which affect the optoelectronic quality of CdTe material. This inhomogeneity may account for the wide spread in the absorption spectra of the CdTe films grown using graphite anode compared to those grown using platinum anode. The post-deposition annealing process may have resulted in the activation and redistribution of the carbon impurities possibly incorporated into CdTe during deposition, most especially as interstitials, resulting in the observed tendency toward p-type conductivity, hence the observed defect property, absorption spectra and solar cell device performance. This detrimental behavior of carbon is attributed to its very small ionic and atomic radii compared to Cd, Te and Pt. The situation can thus result in poor performance of devices fabricated with these contaminated CdTe through the existence of carbon-related carrier trap centres and/or undesirable Fermi level pinning in the CdTe. It therefore becomes important, as a precaution, to use highly inert materials as anodes (counter electrodes) and possibly to avoid graphite anode in the electrodeposition of semiconductors for device application.

Acknowledgement

The principal author would like to thank the Federal University of Technology, Owerri, Nigeria and the University of the Free State, Bloemfontein, South Africa for financial support.

Conflict of interest

Authors declare no conflict of interest and have approved the submission and publication of this manuscript.

References

[1] B. M. Basol, High-efficiency electrodeposited heterojunction solar cell, J. Appl. Phys. 55 (2) (1984) 601 – 603.

[2] D. Cunningham, M. Rubcich and D. Skinner, Cadmium telluride PV module manufacturing at PB Solar, Prog. Photovoltaics: Res. Appl. 10 (2) (2002) 159 – 168.

[3] T. M. Razykov, C. S. Ferekides, D. Morel, E. Stefanakos, H. S. Ullal and H. M. Upadhyaya, Solar Photovoltaic electricity: Current status and future prospects, Solar Energy, 85 (2011) 1580 – 1608.

[4] B. E. McCandless and J. R. Sites, Cadmium telluride solar cells. In Handbook of Photovoltaic Science and Engineering, A. Luque and S. Hegedus (Eds), John Wiley and Sons, Ltd, (2003).

[5] V. B. Patil, D. S. Sutrave, G. S. Shahane and L. P. Deshmukh, Cadmium telluride thin films: growth from solution and characteristics, Thin Solid Films, 401 (1-2) (2001) 35 – 38.

[6] D. G. Diso, F. Fauzi, O. K. Echendu, O. I. Olusola and I. M. Dharmadasa, Optimisation of CdTe electrodeposition voltage for development of CdS/CdTe solar cells, J. Mater. Sci:Mater Electron. 27 (2016). DOI: 10.1007/s10854-016-4844-3

[7] I. M. Dharmadasa, C. J. Blomfield, C. G. Scott, R. Coratger, F. Ajustron and J. Beauvillain, Metal/n-CdTe interfaces: A study of electrical contacts by deep level transient spectroscopy and ballistic electron emission microscopy, Solid-State Electron. 42 (4) (1998) 595 – 604.

[8] C. Heisler, M. Bruckner, F. Lind, C. Kraft, U. Reislohner, C. Ronning and W. Wesh, CdTe grown under Cd/Te excess at very low temperatures for solar cells, J. Appl. Phys. 113 (2013) 224504-1 – 224504-6.

[9] N. R. Paudel, K. A. Wieland and A. D. Compan, Ultrathin CdS/CdTe solar cells by

sputtering, Sol. Energ. Mater.Sol. Cells, 105 (2012) 109 – 112.

[10] J. Britt and C. S. Ferekides, Thin film CdS/CdTe Solar cells with 15.8% efficiency, Appl. Phys. Lett. 62 (1993) 2851 – 2852.

[11] I. M. Dharmadasa, P. A. Bingham, O. K. Echendu, H. I. Salim, T. Druffel, R. Dharmadasa, G. U. Sumanasekera, R. R. Dharmasena, M. B. Dergacheva, K. A. Mit, K. A. Urazov, L. Bowen, M. Walls and A. Abbas, Fabrication of CdS/CdTe-based thin film solar cells using an electrochemical technique, Coatings, 4 (2014) 380 – 415.

[12] M. P. R. Panicker, M. Knaster and F. A. Kroger, Cathodic deposition of CdTe from aqueous electrolytes, J. Electrochem. Soc. 125 (4) (1978) 566 – 572.

[13] S. S. Ou, O. M. Stafsudd and B. M. Basol, Current transport mechanisms of electrochemically deposited CdS/CdTe heterojunction, Solid-State Electron. 27 (1) (1984) 21 - 25.

[14] X. Wu, J. C. Keane, R. G. Dhere, C. Dettart, D. S. Albin, A. Duda, T. A. Gessert, S. Ashar, D. H. Levi and P. Sheldon, 16.5%-efficient CdS/CdTe polycrystalline thin film solar cell, Proceedings of 17th European PVSEC, Munich, Germany, 22 – 26 October (2001) 995 – 1000.

[15] Greentech Media Press Release, First Solar hits 22.1% conversion efficiency for CdTe solar cell, 23 February, 2016. https://www.greentechmedia.com/articles/read/First-Solar-Hits-Record-22.1-Conversion-Efficiency-For-CdTe-Solar-Cell (Accessed on 3 April, 2017).

[16] First Solar Press Release, First Solar achieves world record 18.6% thin film module conversion efficiency, 15 June, 2015. http://investor.firstsolar.com/releasedetail.cfm?ReleaseID=917926 (Accessed on 3 April, 2017).

[17] K. Zanio, Semiconductors and Semimetals, Cadmium Telluride, vol. 13, Academic Press, 1978.

[18] O. K. Echendu, Thin film solar cells using all-electrodeposited ZnS, CdS and CdTe materials, Ph.D thesis, Sheffield Hallam University, United Kingdom, 2014.

[19] O.K. Echendu , F. Fauzi, A.R. Weerasinghea and I.M. Dharmadasa, High short-circuit current density CdTe solar cells using all-electrodeposited semiconductors, Thin Solid Films 556 (2014) 529–534.

[20] O. K. Echendu and I. M. Dharmadasa, Graded-Bandgap Solar Cells Using All-Electrodeposited ZnS, CdS and CdTe Thin-Films, Energies 8 (2015) 4416-4435; doi:10.3390/en8054416.

[21] P. N. Tkachuk, V. I. Tkachuk, V. M. Tsmots and V. S. Shtym, Effect of carbon impurity on the properties of semi-insulating CdTe(Cl) single crystals, Inorganic Materials vol.36 (12) (2000) 1213 – 1216.

[22] I.M. Dharmadasa, Advances in Thin-Film Solar Cells, Boulevard, Singapore, Pan Stanford Publishing Pte. Ltd, (2012) 46.

[23] O. K. Echendu, A. R. Weerasinghe, D. G. Diso, F. Fauzi and I. M. Dharmadasa, Charaterization of n-type and p-type ZnS thin layers grown by an electrochemical method, J. Electron. Mater. 42 (4) (2013) 692 – 700.

[24] S. Tanaka, J. A. Bruce and M. S. Wrighton, Deliberate modification of the behavior of n-type cadmium telluride/electrolyte interfaces by surface etching. Removal of Fermi level pinning, J. Phys. Chem. 85 (1981) 3778 - 3787.

[25] H. S. White, A. J. Rlcco, and M. S. Wrighton, Characterization of p-type CdTe electrodes in acetonitrile/electrolyte solutions. Nearly ideal behavior from reductive surface pretreatments, J. Phys. Chem. 87 (1983) 5140-5150.

[26] Elements atomic radii and the periodic table. http://crystalmaker.com/support/tutorials/crystalmaker/atomic-radii/ (Accessed 25 April, 2017).

[27] O. K. Echendu and I. M. Dharmdasa, the effect on CdS/CdTe solar cell conversion efficiency of the presence of fluorine in the usual $CdCl_2$ treatment of CdTe, Mater. Chem. Phys. 157 (2015) 39 – 44.

[28] I. M. Dharmadasa, O. K. Echendu, F. Fauzi, N. A. Abdul-Manaf, H. I. Salim, T. Druffel, R. Dharmadasa and B. Lavery, Effects of $CdCl_2$ treatment on deep levels in CdTe and their implications on thin film solar cells: a comprehensive photoluminescence study, J. Mater Sci: Mater. Electron. 26 (2015) 4571 – 4583.

[29] I.M. Dharmadasa, J.D. Bunning, A.P. Samantilleke, T. Shen, Effects of multidefects at metal/semiconductor interfaces on electrical properties and their influence on stability and lifetime of thin film solar cells, Sol. Energ. Mater. Sol. Cells (2005) 373 – 384.

[30] M. O. Reese, C. L. Perkins, J. M. Burst, S. Farrell, T. M. Barnes, S. W. Johnston, D. Kuciauskas, T. A. Gessert, and W. K. Metzger, Intrinsic surface passivation of CdTe,

J. Appl. Phys. 118 (2015) 155305-1 – 155305-12.

[31] I.M. Dharmadasa, Recent developments and progress on electrical contacts to CdTe, CdS and ZnSe with special reference to barrier contacts to CdTe Prog. Cryst. Growth & Charact. Mater. 36 (4) (1998) 249 - 290.

[32] A. A. Ojo and I. M. Dharmadasa, 15.3% efficient graded bandgap solar cells fabricated using electroplated CdS and CdTe thin films, Solar Energy 136 (2016) 10–14.

[33] J. P. Ponpon, A review of ohmic and rectifying contacts on cadmium telluride, Solid State Electron. 28 (7) (1985) 689 - 706.

List of figures

Figure 1 : XRD patterns of as-deposited CdTe films grown at different cathodic voltages with (a) graphite anode and (b) platinum anode.

Figure 2: XRD patterns of annealed CdTe films grown with (a) graphite anode and (b) platinum anode.

Figure 3: (111) XRD peak intensity vs. cathodic growth voltage for CdTe grown with (a) graphite anode and (b) platinum anode.

Figure 4: Absorbance vs. photon wavelength for as-deposited CdTe films grown with (a) graphite anode and (b) platinum anode.

Figure 5: Absorbance vs. photon wavelength for annealed CdTe films grown with (a) graphite anode and (b) platinum anode.

Figure 6: Square of absorbance vs. photon energy for as-deposited CdTe films grown with (a) graphite anode and (b) platinum anode.

Figure 7: Square of absorbance vs. photon energy for annealed CdTe films grown with (a) graphite anode and (b) platinum anode.

Figure 8: Proposed Energy band diagrams showing energy level transitions in the photoluminescence measurements of CdTe grown with (a) graphite anode and (b) platinum anode following post-deposition annealing.

Figure 9: Typical SEM images of CdTe films grown using (a) graphite anode and (b) platinum anode.

Figure 10: Typical EDX spectra of CdTe thin films grown on glass/FTO/CdS with (a) graphite anode and (b) platinum anode.

Figure 11: AM 1.5 Current density-voltage graph of g/FTO/CdS/CdTe/Au thin film solar cell fabricated with CdTe grown with (a) graphite anode and (b) platinum anode.